Self-Lubricating Alumina Matrix Composites

7

Ashish K. Kasar and Pradeep L. Menezes

Contents

7.1 Introduction 202
7.2 Soft Materials 204
7.3 Lamellar Solids 205
7.4 Other Compounds 210
7.5 Conclusions 215
References 215

Abstract

Alumina is a widely used ceramic for tribological applications such as gears, bushings, bearings, etc. due to its chemical and physical stability. However, the friction between alumina-alumina is high, which reduces its usage for tribological applications. To overcome the high friction, various solid lubricants can be added in the alumina matrix that makes self-lubricating alumina composites. In this chapter, mainly three categories of solid lubricants: soft material, lamellar solids, and other materials (oxides, sulfates, etc.) used in alumina matrix are discussed. Mostly, these solid lubricants form a tribo-layer at the interface between alumina composite and counterpart and reduce friction. The amount of solid lubricants needs to be optimized because the excessive amount can cause severe wear that can damage the dimensional stability of the component. While discussing the suitable solid lubricants for the alumina matrix, various synthesis techniques have also been highlighted because synthesis techniques are critical to disperse the solid lubricants uniformly.

A. K. Kasar
Mechanical Engineering Department, University of Nevada, Reno, NV, USA

P. L. Menezes (✉)
Department of Mechanical Engineering, University of Nevada, Reno, NV, USA
e-mail: pmenezes@unr.edu

P. L. Menezes et al. (eds.), *Self-Lubricating Composites*,
https://doi.org/10.1007/978-3-662-64243-6_7

7.1 Introduction

Ceramics are nonorganic solid material that consists of metal or nonmetal compounds with ionic or covalent bonds. Ceramic materials contain a combination of properties, including low density, resistance to chemicals, high wear resistance, and stability for a wide temperature range. Due to these properties, structural ceramic materials have the potential to be utilized in the tribological applications. These structural ceramic materials have a wide range of compounds including oxides, carbides, nitrides, and borides.

However, the major limitation of structural ceramics is the high coefficient of friction (COF) for tribological applications. Self-lubricating ceramic composites have suitable tribological properties, especially for high-temperature applications, where a lubricious layer of solid lubricant (SL) materials forms at the interface during sliding that can significantly reduce the energy loss due to friction. Interestingly, some oxide ceramics act as SL materials that can be added in the ceramics to form self-lubricating ceramic composites. These solid lubricating oxide materials are listed in Table 7.1.

The self-lubrication performance of ceramic composites depends on the formation of transfer film of SL at the interface. The transfer film formation is controlled by many factors including volume/weight fraction of SL (inclusion), mechanical properties of the SL, and operating conditions of tribo-contact. For example, the higher transfer film thickness is expected by increasing the volume fraction of SL or by choosing the softer solid particles as predicted by a mathematical model for 3 mol% yttria-doped zirconia (3Y-TZP) [1]. In this model, fair assumptions were taken by considering the elastic deformation of the matrix whereas graphite deforms plastically to de-bond with the matrix and form the transfer layer. The predicted transfer layer thickness by varying the volume fraction and considering the variation in yield strength of the SL phase (inclusions) are shown in Fig. 7.1. However, the SLs in the ceramic matrix can only be loaded up to a critical amount. The critical amount of the SL phase in the ceramic matrix can be evaluated by friction performance along with wear rate/volume, mechanical strength, and other required properties of the composites. Experimentally, Xue et al. [2] observed that 24.4 vol% graphite content in the ZrO_2 (Y_2O_3 mol%) reduced COF from 0.56 to 0.29 against GCr15 steel whereas the wear increased from 5.8×10^{-6} to 8×10^{-5} mm^3m^{-1}. Therefore, it is essential to optimize the SL amount in the matrix based on other required properties.

Table 7.1 Categories of SL materials

Soft materials	Lamellar solids	Organic polymers	Other compounds (oxides, sulfates, and phosphates)
Bi, Ag, Cu, Sn, In, Pb, CaF_2, BaF_2, PbS	MoS_2, WS_2, h-BN, graphite.	PTFE, nylon, waxes	TiB_2, B_2O_3, MoO_2, MoO_3, ZnO_2, Re_2O_7, TiO_2, Ag_2O, CuO, $BaSO_4$

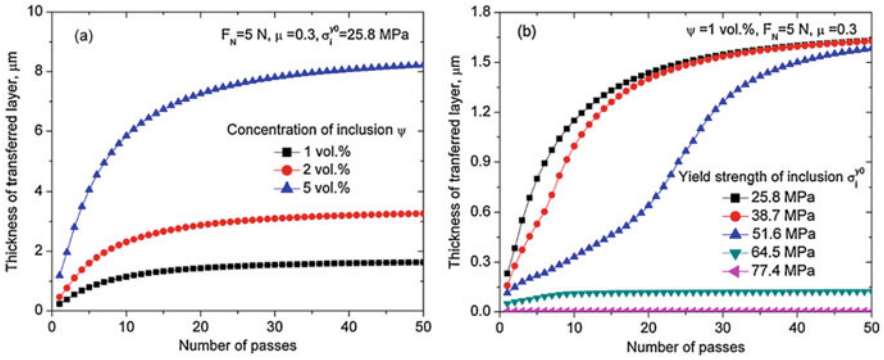

Fig. 7.1 Predicted transfer layer thickness for ceramic composite using a model [1]

Table 7.2 Properties of Al_2O_3 ceramic [9]

Properties	Value
Density	3.95 g/cm^3
Melting point	2050 °C
Yield strength	455 MPa
Elastic modulus	380 GPA
Thermal conductivity	40 W/m.K
Coefficient of thermal expansion	8.0×10^{-6}/°C

This chapter reviews the studies on tribological performance of Al_2O_3 matrix self-lubricating composites. Alumina is the most common ceramic materials which employed at high temperature for various applications due to its high-temperature stability, lower density, high hardness, and being chemically inert. The physical and mechanical properties of the alumina are listed in Table 7.2. However, the friction and wear performance of alumina is poor under the dry sliding condition that limits the applicability for tribological applications. To overcome the poor tribological performance of alumina, coatings of SLs materials have been provided, such as polytetrafluoroethylene (PTFE) [3], Ag [4, 5], TiB_2 [6–8], etc. Coating of these SL materials provides lower friction, whereas hard alumina base acts as a wear-resistance substrate to support the soft and shearing SL phases. This chapter is focused on understanding the tribological performance of alumina composite reinforced with SLs rather than the coating of SL materials.

In this chapter, the sections are divided based on the different categories of SLs described in Table 7.1 which are soft material, lamellar solids, and other compounds (oxides and sulfates). The organic polymers are excluded because these have not been used widely as a lubricating material in Al_2O_3 matrix. On the contrary, alumina has been used as a reinforcement material in polymers [10–13]. The feasibility of the various SLs from the rest three categories in Al_2O_3 matrix at different working conditions is evaluated by understanding the mechanism. Often, SLs, in combination

with different categories, are used for superior lubrication. Such studies have been assigned to subsections based on the most effective SL observed in the study.

7.2 Soft Materials

CaF_2 is the most common soft SL material, which is often used as SL in ceramic matrix composites. The Al_2O_3-CaF_2 composites can be synthesized by different methods. For example, the laser-cladded Al_2O_3-30 wt% CaF_2 coating on Al_2O_3 showed improved friction and wear properties compared to monolithic laser-cladded Al_2O_3 [14]. The Al_2O_3 showed a COF of 0.6, whereas the composite showed COF of 0.48 when tested against hardened steel on the pin-on-wheel test setup with a normal load of 98 N at room temperature. The composite showed 40 times lesser wear compared to monolithic laser-cladded Al_2O_3. The improved tribological performance was observed due to uniform distribution of the soft spherical CaF_2 phase in the plate-like framework of Al_2O_3 phase. The lower amount of CaF_2 (3 wt%) was also observed to improve tribological properties of Al_2O_3-ZrO_2 (15 wt%) composite prepared by the plasma spray method [15]. The COF was reduced upto 40%. Also, the observed wear rate was four times lower at 20 N as compared with those of composites without CaF_2. In this study, 3 mol% Y_2O_3-stabilized ZrO_2 was added in Al_2O_3 matrix, which forms eutectic ceramic composites, and it is well known to improve the mechanical properties of Al_2O_3 [16–18].

Similar to CaF_2, BaF_2 and SrF_2 are also considered a soft phase that can act as SLs. Murakami et al. [19] investigated the three different composites: Al_2O_3–31BaF_2–19CaF_2, Al_2O_3–50CaF_2, and Al_2O_3–50SrF_2 (mass %) that were synthesized by spark plasma sintering and tested at 600 °C against alumina ball with a normal load of 4.9 N. Among all the composites, Al_2O_3–31BaF_2–19CaF_2 showed the best tribological performance with 0.3–0.4 COF and wear rate of the composite was 0.8×10^{-5} mm^3/N.m. The Al_2O_3–31BaF_2–19CaF_2 composite also showed 4 GPa of microhardness that is two times higher than the hardness of other alumina composites. The SL phases provided lower friction and wear but also resulted in finer microstructure that improves hardness. This suggests that the combination of SL phases in the alumina matrix can outperform a single SL.

Secondary hard phases such as ZrO_2, TiC, SiC, and TiN, etc. have also been added in the alumina matrix along with SL materials. The purpose of secondary hard phases is to strengthen the composite by whisker, precipitate, and dispersion strengthening. For example, Al_2O_3/TiC composite with CaF_2 showed improved tribological and mechanical properties [20]. These composites were prepared by hot pressing at 36 MPa in N_2 atmosphere for 15 min at 1700 °C. The composition and properties of the composites are listed in Table 7.3. Table 7.3 indicates that the mechanical properties (flexure strength and hardness) deteriorated with the addition of SL CaF_2, whereas the COF and wear rate reduced till 10 vol% of CaF_2. Therefore, Al_2O_3/TiC/15%CaF_2 composite provides optimized mechanical and tribological properties. In this work, properties were not compared with respect to monolithic

Table 7.3 Mechanical and tribological properties of Al_2O_3/TiC/CaF_2 composites

Composition (vol%) Al_2O_3: TiC = 1:1	Flexure strength (MPa)	Hardness (GPa)	COF	Wear rate (10^{-5} mm^3/N.m)
Al_2O_3 + TiC	800	20	0.47	2.7
Al_2O_3 + TiC + 5% CaF_2	478	13.2	0.31	2.5
Al_2O_3 + TiC + 10% CaF_2	590	15.3	0.27	1.8
Al_2O_3 + TiC + 15% CaF_2	418	9.6	0.30	3.5

Al_2O_3. However, TiC is expected to enhance the mechanical properties of Al_2O_3, whereas CaF_2 provided self-lubrication.

7.3 Lamellar Solids

Carbonaceous material such as graphite, graphene, and carbon nanotubes (CNTs) have been extensively studied for tribological applications due to their lamellar structure [21–26]. These carbonaceous materials have also been utilized in the alumina matrix. Bagde et al. [27] studied Al_2O_3-13TiO_2-15% Ni-graphite coatings deposited by plasma spray. The tribological tests were carried out against 21 and 36 μm SiC papers. The observed friction and wear results are shown in Fig. 7.2a, b, respectively. It can be seen that the addition of Ni-graphite reduced the COF at all the loads against both the SiC papers. The effect of Ni-graphite is higher on the wear rate as it reduced by 1.5–2 times. A similar effect of Ni-graphite on the Al_2O_3-SiO_2 plasma sprayed coating was observed where graphitic lubricating layers reduced friction at the interface, and the ceramic matrix worked as a load-bearing element [28].

Similar to graphite, graphene has also been found to form tribo-layer during sliding in Al_2O_3-graphene composites [29, 30]. Al_2O_3-0.22 wt% graphene composites were prepared by spark plasma sintering at 80 MPa and 1500 °C [29]. The tribological tests against Al_2O_3 ball at 20 N showed ~10% and 50% decrease in COF and wear rate for graphene composite with respect to pure Al_2O_3 sample. The formation of a uniform tribo-layer of graphene was observed by Zhang et al. in Al_2O_3-graphene nanoplatelet composite synthesized by spark plasma sintering [30]. The authors observed optimum tribological performance with 0.5 vol% graphene nanoplatelet with 65 and 25% decrease in wear volume and friction coefficient, respectively, with respect to pure Al_2O_3. Graphene content higher than the optimum amount showed higher wear. Graphene oxide, which contains oxygen-carrying groups such as -OH, -COOH, etc., on the edges of graphene sheets [23], has also been found effective to improve the tribological performance of Al_2O_3. Al_2O_3-graphene oxide composite synthesized by spark plasma sintering resulted in five times lower wear compared to monolithic alumina tested against alumina ball at 10 N normal load [31]. However, a detailed study on graphene and graphene oxide-Al_2O_3 composite suggests that unoxidized graphene provides superior mechanical properties than the graphene oxide and reduced graphene oxide [32]. It is due to the

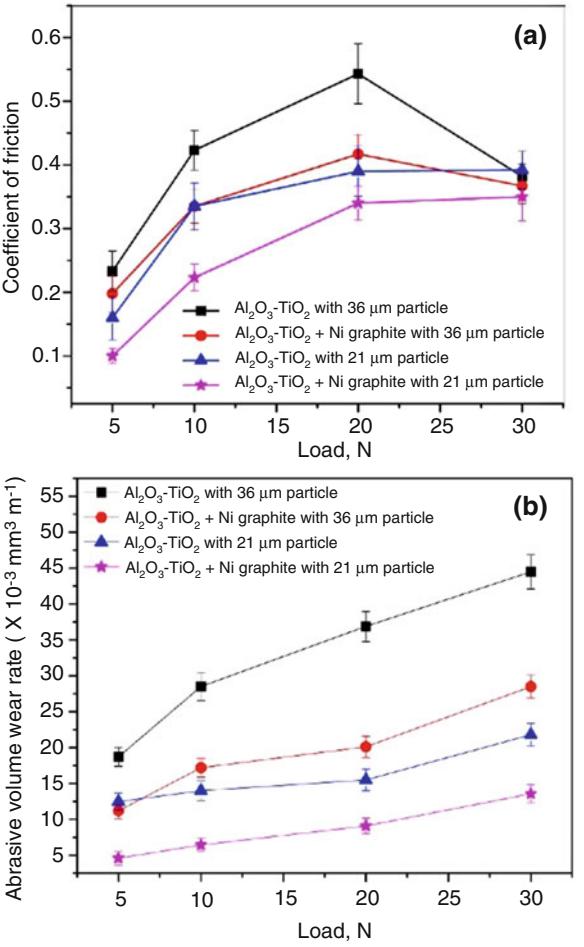

Fig. 7.2 (**a**) COF and (**b**) wear rate of Al_2O_3-13TiO_2 and Al_2O_3-13TiO_2 + Ni graphite composite against 21 and 36 μm SiC abrasive surfaces [27]

presence of structural defects in graphene oxide and reduced graphene oxide that can deteriorate the mechanical properties of the composite. The wear and friction data of Al_2O_3-unoxidized graphene is shown in Fig. 7.3, where unoxidized graphene is denoted by EG and LPS denotes liquid phase sintering. It can be seen that the wear rate of the graphene-containing composite reduced by one order of magnitude and friction was reduced by 15–20% compared to pure Al_2O_3. Other than the tribological properties, the addition of graphene in Al_2O_3 matrix led to the improvement in mechanical [33–35] and different functional properties [36, 37].

The other attractive carbonaceous material is carbon nanotubes (CNTs). CNTs have also been employed in the Al_2O_3 matrix. Al_2O_3-CNTs composite synthesized by hot pressing at 1800 °C under 40 MPa. The Al_2O_3-CNTs composite showed improved mechanical and tribological performance as compared to pure Al_2O_3

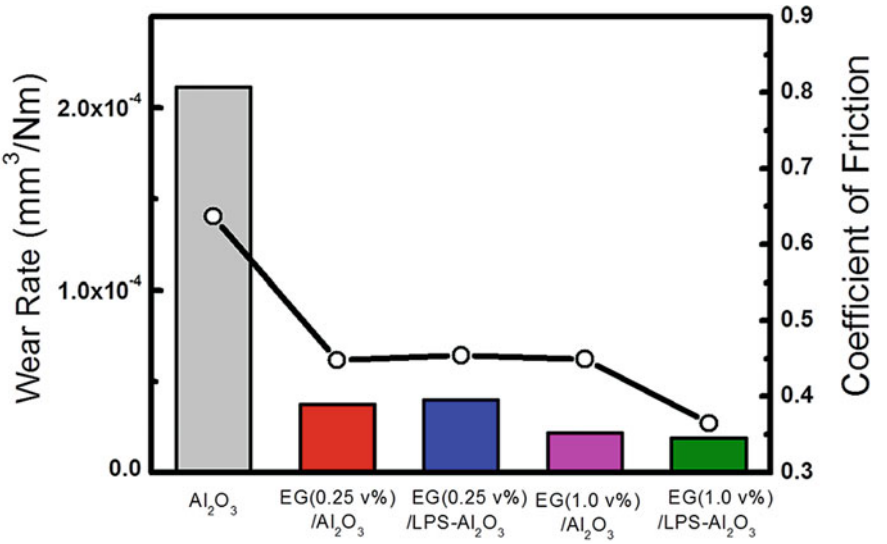

Fig. 7.3 Wear rate and COF for Al_2O_3-unoxidized graphene (EG) tested against WC ball at 25 N with 10 cm/s sliding speed for 2000 m [32]

[38]. The effect of CNTs concentration on the microhardness of the composites is shown in Fig. 7.4a. The highest microhardness was observed for 4 wt% CNTs in the alumina matrix. Any further addition of CNTs led to a reduction in hardness due to inhomogeneous dispersion of CNTs. The tribological tests were carried out using silicon nitride ball as a counterpart at 25 N and 10 mm/s sliding velocity. Figure 7.4b shows the variation in COF and wear with respect to CNTs content. It can be seen that the Al_2O_3-CNTs composite with 4 wt% yielded least wear loss with COF of 0.43. The composite with 12.5% CNTs provided the lowest COF of 0.3 but higher wear rate, which is more than two times of pure alumina. Similar behavior was also observed by Lim et al. who showed an increase in wear rate with CNTs content for hot-pressed Al_2O_3-CNTs composite (Fig. 7.5a) [39]. The authors also prepared the composite by tape casting other than hot pressing. In tape casting, the ceramic slurry was cast in thin layers followed by drying. These layers were laminated by hot pressing. The resulted composite showed a reduction in wear loss with the increase in CNTs content while maintaining the same friction coefficient (Fig. 7.5a, b). In this study, the tribological tests were performed against silicon nitride ball at 25 N load with 10 mm/s sliding speed. The tape casting method allowed to disperse higher amount of CNTs in alumina to achieve superior tribological and mechanical properties.

The other lamellar SLs are MoS_2, BN which have been used as reinforcements in various metallic and ceramic materials, including alumina. For example, Su et al. [40] prepared the Al_2O_3/MoS_2 composite by in situ syntheses of MoS_2 in the porous Al_2O_3 matrix. The porous Al_2O_3 matrix was developed by sintering the green body made of Al_2O_3 and graphite (10 vol%), the graphite oxidized during sintering in air

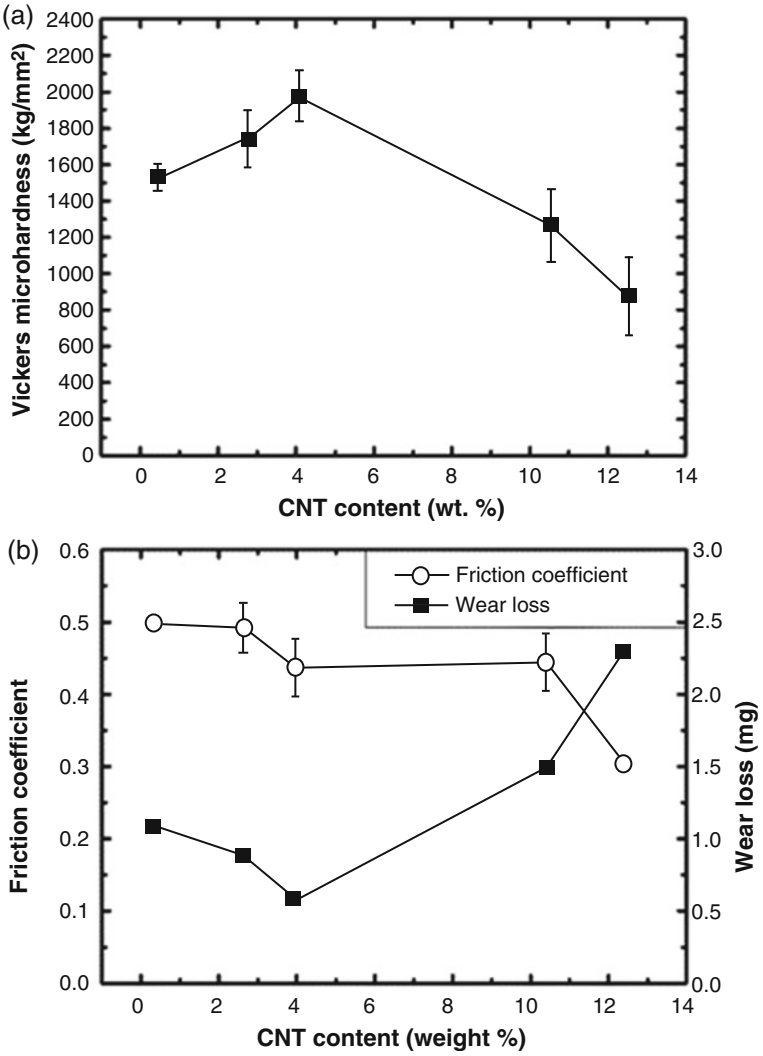

Fig. 7.4 (**a**) Microhardness, (**b**) COF and wear loss of the Al_2O_3-CNTs composite [38]

and led to formation of pores. After sintering, the porous sample was immersed in a solution that consists of sodium molybdate, thiourea, and deionized water under vacuum. After vacuum infusion, the porous samples immersed in solution were heated at 220 °C in stainless steel autoclave for 56 h. This hydrothermal process led to the formation of MoS_2 in the pores of the sintering Al_2O_3 matrix. The tribological property of resulted composite was tested against Si_3N_4 ball in a vacuum environment ($<5.0 \times 10^{-5}$ mbar) at 5 N normal load. The COF of the composite (0.2) was reduced significantly compared to sintered Al_2O_3 sample (0.75) as shown in Fig. 7.6a. At the same time, three orders of magnitude reduced wear rate due to the formation of MoS_2 film at the interface. EDS on wear track of Al_2O_3-MoS_2

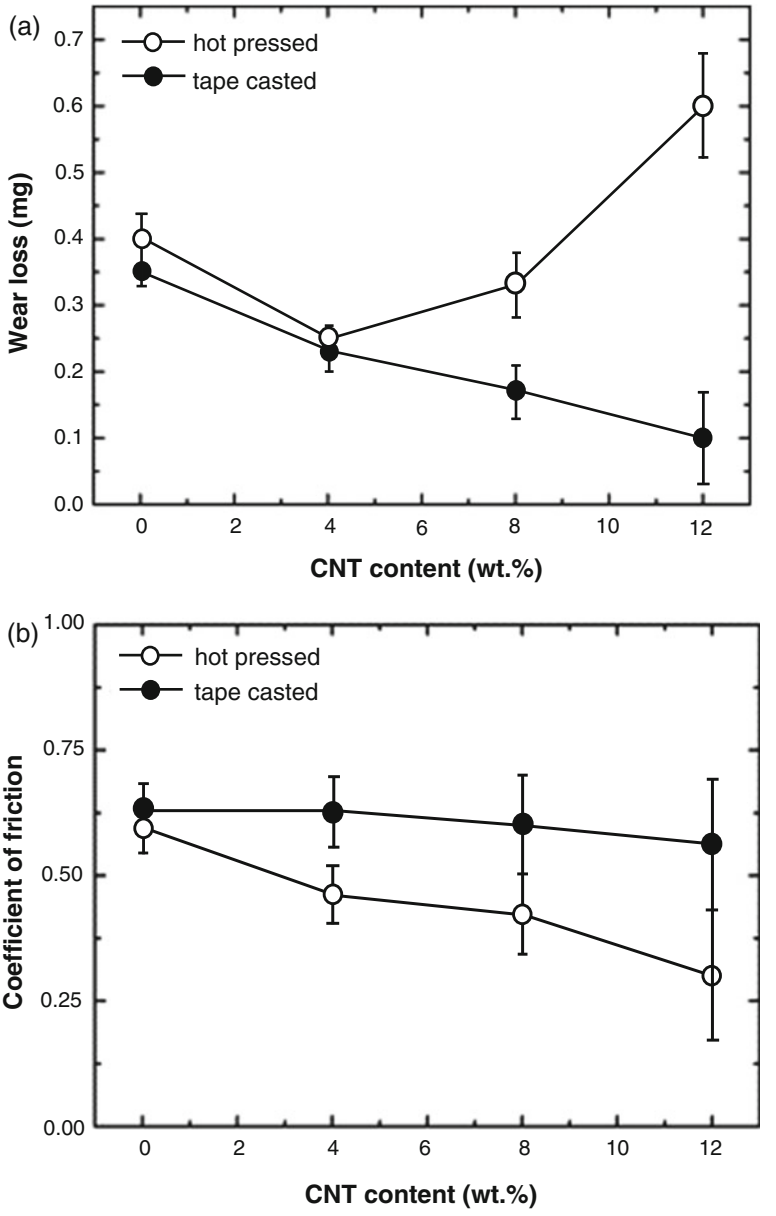

Fig. 7.5 The effect of CNTs content on (**a**) wear loss and (**b**) COF of Al_2O_3-CNTs composite synthesized by hot pressing and tape casting method [39]

composite (Fig. 7.6c) showed the presence of Mo and S, which were not present on the wear track of Al_2O_3 (Fig. 7.6a).

The combination of two lamellar SLs MoS_2, BN on mechanical properties was investigated by Deng et al. [41]. The composites were prepared using these lamellar

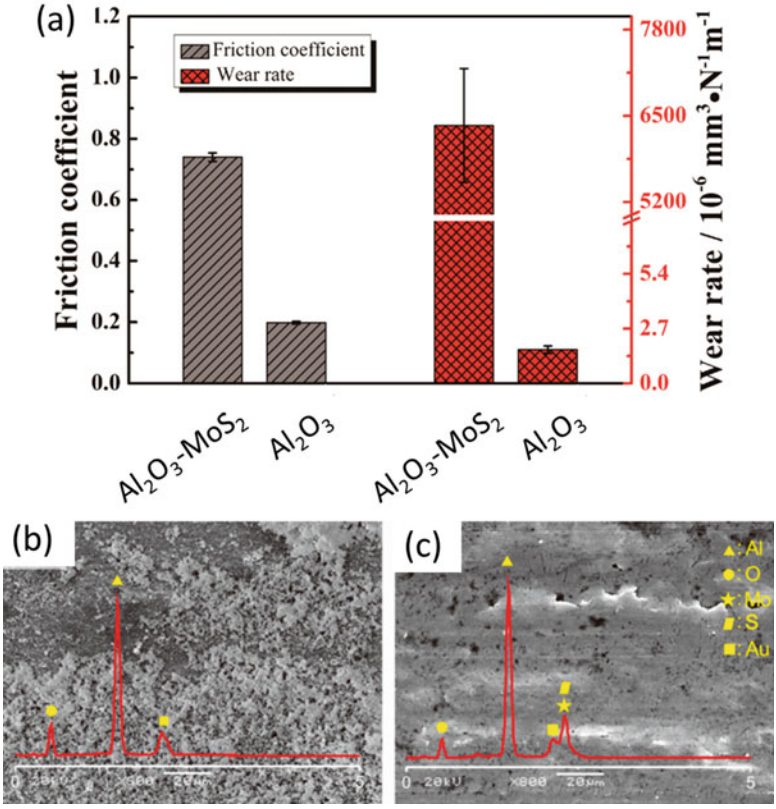

Fig. 7.6 (**a**) Friction and wear rate of Al_2O_3-MoS_2 composite, (**b**) and (**c**) are wear track of Al_2O_3 and Al_2O_3-MoS_2 composite, respectively [40]

solids (5, 10, and 15 vol%) in the Al_2O_3-TiC matrix (1:1 vol ratio) by hot pressing in an argon atmosphere for 15 min at 1700 °C. For all the composites, hardness and fracture toughness reduced with an increase in SL content. With 15 vol% of MoS_2, the hardness and fracture toughness were reduced by 2.1 and 1.73 times, respectively, whereas 15 vol% of BN reduced the same by 8.7 and 2.6 times with respect to the Al_2O_3-TiC matrix. These results support that the addition of SLs cause a reduction in mechanical properties. However, a hard phase such as TiC or SiC can be added in the alumina matrix to compensate for the loss in mechanical properties.

7.4 Other Compounds

In this section, other SL compounds such as sulfates and oxides are included. The most common SL sulfates are $BaSO_4$. Murkami et al. [42] studied the Al_2O_3 reinforced with $BaSO_4$ SL. The Al_2O_3-50% $BaSO_4$ composites were prepared by

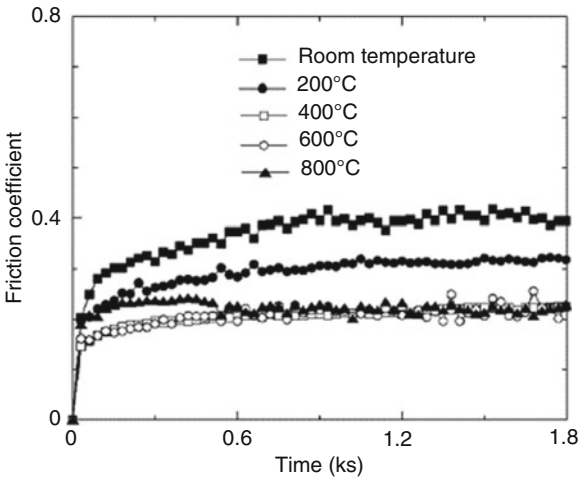

Fig. 7.7 Friction coefficient of Al_2O_3-50$BaSO_4$-20Ag against alumina ball at different temperatures [43]

spark plasma sintering. The tribological tests against Al_2O_3 ball were conducted at up to 800 °C. The composite was able to retain a COF between 0.2 and 0.4 over the temperature range. The lower friction was due to the formation of $BaSO_4$ film at the interface. An extension to this study, the same research group investigated the tribological performance of Al_2O_3-50$BaSO_4$-20Ag, Al_2O_3-50$BaSO_4$-10SiO_2, Al_2O_3-50$SrSO_4$, and Al_2O_3-50$PbSO_4$-5SiO_2. Among all the composites, Al_2O_3-50$BaSO_4$-20Ag showed the least COF. At the temperature range of 400–800 °C, the COF for Al_2O_3-50$BaSO_4$-20Ag was 0.2, as shown in Fig. 7.7. The micrographs of wear tracks are shown in Fig. 7.8. Ag tribo film was observed on the wear track of the samples tested at 400 °C and above that reduced the COF to 0.2. The authors also stated that the $BaSO_4$ has a barite-type structure that can be cleaved along (0 0 1), which results in lower COF. Also, the $BaSO_4$ becomes ductile above 400 °C that can further enhance the self-lubrication behavior.

The effect of different oxides on the tribological behavior of alumina composites was investigated by Kerkwijk et al. [44]. The different alumina composites with 5 wt% of MgO, CuO, MnO_2, and B_2O_3 reinforcement were synthesized by isostatic pressing at 400 MPa. The green pellets after isostatic pressing was sintered at 1500 °C for 2 h. The sliding tests were conducted against alumina ball at room temperature with a 10 N normal load. The composites with MnO_2, MgO, and B_2O_3 showed mean COF values of 0.48, which is lower than the other composites and pure alumina (0.55). For the composites with CuO and ZnO, the observed COF are 0.65 and 0.49, respectively. The addition of oxides other than CuO resulted in lowering the friction of alumina from 0.55 to ~0.48. These ceramic composites also showed low specific wear rates, in the range of 10^{-9} to 10^{-8} mm^3/Nm.

Al_2O_3 is also used as a cutting tool where friction and wear are important parameters for the tool's performance and life. These tools can be reinforced with

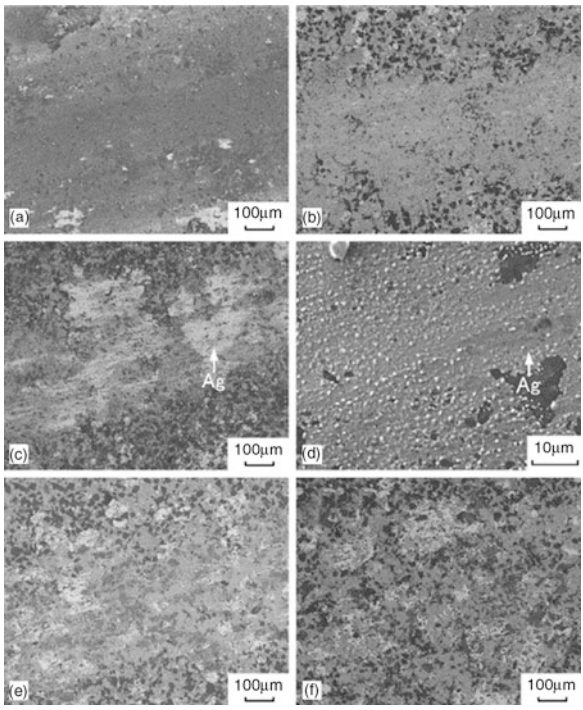

Fig. 7.8 Wear track of Al_2O_3-50$BaSO_4$-20Ag at (**a**) room temperature, (**b**) 200 °C, (**c**, **d**) 400 °C, (**e**) 600 °C, and (**f**) 800 °C [43]

SLs, for example, Al_2O_3-TiB_2 ceramic cutting tools were synthesized with different TiB_2 content (10–40 vol%) by hot pressing and tested through dry high-speed machining on hardened steel while measuring friction, wear, and cutting speed [8]. It was found that both wear and COF at the tool–chip interface were reduced with increase in sliding speed and TiB_2 content. The composite with 40 vol% resulted in a COF of 0.2, which was ~42% lower than the composite with 10 vol% TiB_2. The cutting speed during the experiment was 200 m/min. Flank wear was also reduced for Al_2O_3-40 vol% TiB_2 and it was 30–40% lesser than the Al_2O_3-10 vol% TiB_2 composite. The observed lower COF and wear was due to the formation of a self-lubricating oxide film (TiO_2) at the tool–chip interface because of the tribological chemical reaction at the elevated cutting temperature. The mechanism was confirmed by carrying out the same cutting process in a nitrogen atmosphere where no oxides were performed, and wear was significantly higher.

In addition to uniform reinforcement of SLs, laminated alumina composites have been studied to improve mechanical properties along with tribological properties. The laminated ceramic structure is inspired by structures available in nature, such as shells, lignum, or teeth that show improved failure behavior in comparison with monolithic ceramic material. Qi et al. [45] prepared the laminated structure of Al_2O_3/Mo by powder metallurgy route by stacking the alternate layers of ball-milled powders in a mold followed by hot pressing at 1550 °C and 25 MPa for 90 min in

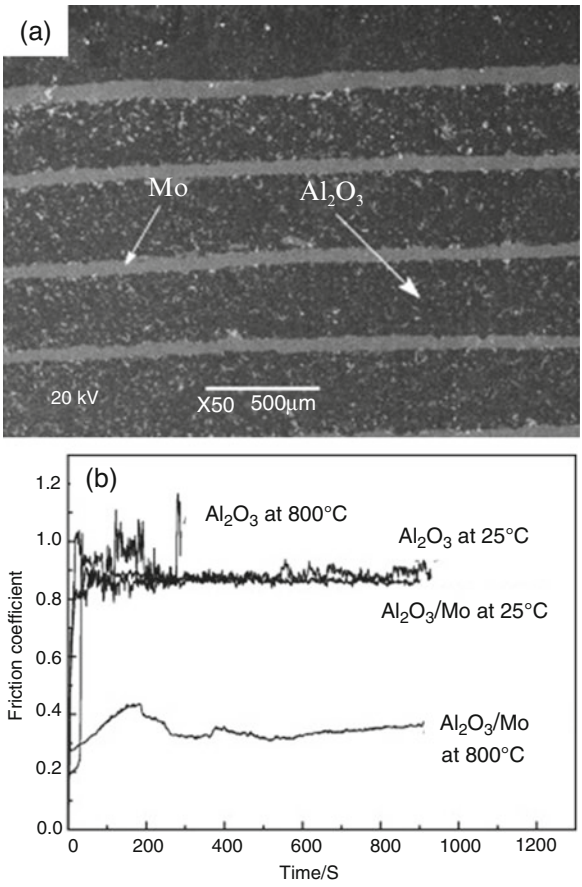

Fig. 7.9 (**a**) SEM micrograph of Al_2O_3/Mo-laminated composites and (**b**) friction coefficients of Al_2O_3/Mo-laminated composites and monolithic Al_2O_3 ceramics at 25 and 800 °C [45]

an inert atmosphere of Ar. The SEM micrograph of Al_2O_3/Mo-laminated composites is shown in Fig. 7.9a. The laminated structure showed improved fracture toughness of 9.14 MPa $m^{1/2}$ compared with fracture toughness of monolithic alumina that is 5.69 MPa $m^{1/2}$. The tribological performance of the structure was tested at 25 and 800 °C against the alumina pin at 70 N. The friction coefficient is shown in Fig. 7.9b. At room temperature, the laminated structure showed the same friction as the monolithic alumina. However, a drastic decrease in friction from 0.9–0.4 can be observed at 800 °C for the laminated structure. The reduction in COF was due to the formation of molybdenum oxides (MoO_2 and $MoO_{2.8}$) observed by XRD on the wear track. The plastic deformation ability of molybdenum oxides provided the laminated structure self-lubricating properties at high temperature.

A further change in design to improve the self-lubricity of the Al_2O_3-Mo-laminated structure was carried out by Zhang et al. [46], where laser surface texture was created on the laminated structure as shown in Fig. 7.10a. The SLs materials, MoS_2

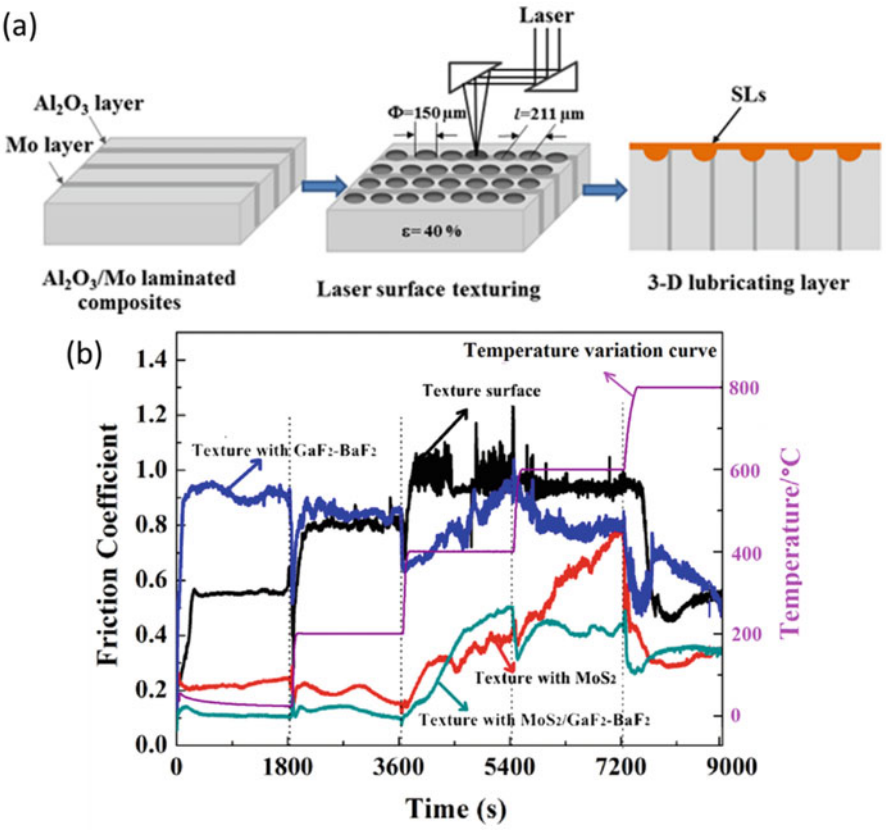

Fig. 7.10 (**a**) Schematic of fabricating Al_2O_3/Mo-laminated composite with laser texturing + SLs, and (**b**) COF of the laminated structure with burnished SLs at different temperatures [46]

and CaF_2–BaF_2, were burnished on the textured surface. The tribological performance of the prepared structure was tested against alumina pin from room temperature to 800 °C. The observed COF trends are shown in Fig. 7.10b. Figure 7.10b shows that the composite structure containing MoS_2 had lower friction coefficient of 0.1–0.2 from room temperature to 200 °C. Whereas, the composite with CaF_2-BaF_2 had higher friction at room temperature. At 600 °C, composite with MoS_2 showed higher friction compared to the composite with combination of MoS_2 and CaF_2-BaF_2. It suggests that MoS_2 reduces friction at lower temperatures, whereas CaF_2-BaF_2 helps to maintain lower friction at the higher temperature range. Therefore, the combination of these SLs is preferable. The lower friction is due to the transfer film of MoS_2 and in situ formed oxides. The formation of MoO_2 is explained in the previous paragraph. The MoO_2 was also reacted with CaF_2-BaF_2 to form $CaMoO_4$ and $BaMoO_4$ during sliding at the higher temperature and improve high-temperature lubrication.

7.5 Conclusions

In this chapter, SLs have been characterized based on their nature, such as soft material, which is easy to deform that can reduce friction at the interface. The SLs are discussed mainly for the alumina matrix for room temperature and high-temperature applications. It has also shown that the combination of SLs from different categories have been effective at different temperature range, such as CaF_2 is mainly suitable for high-temperature application whereas graphite and MoS_2 work well even at room temperature in the alumina matrix.

Self-lubrication nature of the alumina composites is governed by the formation of continuous tribo-layer at the interface that minimizes the contact between counter bodies and reduces friction. However, the addition of SLs in alumina is decided by two factors: (i) excessive amount can cause nonuniform dispersion and (ii) excessive amount can increase wear drastically. The nonuniform dispersion of SLs can be taken care of by suitable synthesis techniques or prior colloidal mixing. However, the severe wear can be controlled by optimizing the amount of SLs based on the application parameters, such as load, velocity, roughness, and properties of the counterpart.

Other than conventional reinforced alumina composites, laminated structures of alumina have also been developed with Mo, where the formation of MoO_2 provided lower friction. Further enhancement on this laminated structure has been carried out by the formation of small grooves using laser treatment. These grooves acted as a sink for SLs materials for the continuous formation of tribo-layer. Overall, it has been seen that alumina is compatible with all the SLs without the formation of any unwanted chemical compound. The inherent properties of alumina combined with SLs make the composite suitable for tribological applications at extreme environments.

Funding The authors appreciate the funding from NASA CAN, grant number NV-80NSSC20M0221.

References

1. Song, J., Valefi, M., de Rooij, M., Schipper, D.J.: A mechanical model for surface layer formation on self-lubricating ceramic composites. Wear. **268**(9), 1072–1079 (2010). https://doi.org/10.1016/j.wear.2010.01.012
2. Liu, H., Xue, Q.: The tribological properties of TZP-graphite self-lubricating ceramics. Wear. **198**(1), 143–149 (1996). https://doi.org/10.1016/0043-1648(96)06946-3
3. Wang, Z., Wu, L., Qi, Y., Cai, W., Jiang, Z.: Self-lubricating Al_2O_3/PTFE composite coating formation on surface of aluminium alloy. Surf. Coat. Technol. **204**(20), 3315–3318 (2010). https://doi.org/10.1016/j.surfcoat.2010.03.049
4. Putyra, P., Podsiadło, M., Smuk, B.: Alumina composites with solid lubricant content. J. Achiev. Mater. Manuf. Eng. **41**(1-2), 34–39 (2010)
5. Jin, Y., Kato, K., Umehara, N.: Effects of sintering aids and solid lubricants on tribological behaviours of CMC/Al_2O_3 pair at 650°C. Tribol. Lett. **6**(1), 15–21 (1999)
6. Masanta, M., Shariff, S.M., Choudhury, A.R.: Tribological behavior of TiB_2–TiC–Al_2O_3 composite coating synthesized by combined SHS and laser technology. Surf. Coat. Technol. **204**(16), 2527–2538 (2010). https://doi.org/10.1016/j.surfcoat.2010.01.027
7. Jianxin, D.: Friction and wear behaviour of Al_2O_3/TiB_2/SiCw ceramic composites at temperatures up to 800 C. Ceram. Int. **27**(2), 135–141 (2001)

8. Jianxin, D., Tongkun, C., Lili, L.: Self-lubricating behaviors of Al_2O_3/TiB_2 ceramic tools in dry high-speed machining of hardened steel. J. Eur. Ceram. Soc. **25**(7), 1073–1079 (2005)
9. Taylor, A.: Ceramics – Materials, Joining and Applications. https://www.twi-global.com/technical-knowledge/job-knowledge/ceramics-materials-joining-and-applications-054.aspx (2020). Accessed 10 July 2020
10. Burris, D.L., Sawyer, W.G.: Tribological sensitivity of PTFE/alumina nanocomposites to a range of traditional surface finishes. Tribol. Trans. **48**(2), 147–153 (2005)
11. Xiang, D., Li, K., Shu, W., Xu, Z.: On the tribological properties of PTFE filled with alumina nanoparticles and graphite. J. Reinf. Plast. Compos. **26**(3), 331–339 (2007)
12. Guglani, L., Gupta, T.: Wear and mechanical properties of nylon 66–Al_2O_3 microcomposite. J. Reinf. Plast. Compos. **36**(17), 1254–1262 (2017)
13. Saravanan, D., Palanisamy, C., Raajeshkrishna, C.: Tribological performance of multi walled carbon nanotubes–alumina hybrid/epoxy nanocomposites under dry sliding condition. Mater. Res. Express. **6**(10), 105067 (2019)
14. Wang, H.M., Yu, Y.L., Li, S.Q.: Microstructure and tribological properties of laser clad CaF_2/Al_2O_3 self-lubrication wear-resistant ceramic matrix composite coatings. Scr. Mater. **47**(1), 57–61 (2002). https://doi.org/10.1016/S1359-6462(02)00086-6
15. Kim, S.H., Hannula, S.P., Lee, S.W.: Effects of the sliding conditions on the tribological behavior of atmospheric plasma sprayed Al_2O_3–15wt.% ZrO_2–CaF_2 composite coating. Surf. Coat. Technol. **210**, 127–134 (2012). https://doi.org/10.1016/j.surfcoat.2012.09.003
16. Sarkar, D., Adak, S., Mitra, N.: Preparation and characterization of an Al_2O_3–ZrO_2 nanocomposite, part I: powder synthesis and transformation behavior during fracture. Compos. A: Appl. Sci. Manuf. **38**(1), 124–131 (2007)
17. Wang, C.-J., Huang, C.-Y., Wu, Y.-C.: Two-step sintering of fine alumina–zirconia ceramics. Ceram. Int. **35**(4), 1467–1472 (2009)
18. Niu, F., Wu, D., Ma, G., Wang, J., Guo, M., Zhang, B.: Nanosized microstructure of Al_2O_3–ZrO_2 (Y_2O_3) eutectics fabricated by laser engineered net shaping. Scr. Mater. **95**, 39–41 (2015)
19. Murakami, T., Ouyang, J.H., Sasaki, S., Umeda, K., Yoneyama, Y.: High-temperature tribological properties of Al_2O_3, Ni–20mass% Cr and NiAl spark-plasma-sintered composites containing BaF_2–CaF_2 phase. Wear. **259**(1), 626–633 (2005). https://doi.org/10.1016/j.wear.2004.12.019
20. Deng, J., Liu, L., Yang, X., Liu, J., Sun, J., Zhao, J.: Self-lubrication of $Al_2O_3/TiC/CaF_2$ ceramic composites in sliding wear tests and in machining processes. Mater. Des. **28**(3), 757–764 (2007)
21. Dorri Moghadam, A., Omrani, E., Menezes, P.L., Rohatgi, P.K.: Mechanical and tribological properties of self-lubricating metal matrix nanocomposites reinforced by carbon nanotubes (CNTs) and graphene – a review. Compos. Part B. **77**, 402–420 (2015). https://doi.org/10.1016/j.compositesb.2015.03.014
22. Kasar, A.K., Menezes, P.L.: Synthesis and recent advances in tribological applications of graphene. Int. J. Adv. Manuf. Technol. **97**(9-12), 3999–4019 (2018)
23. Kasar, A.K., Xiong, G., Menezes, P.L.: Graphene-reinforced metal and polymer matrix composites. JOM. **70**(6), 829–836 (2018)
24. Tan, H., Wang, S., Yu, Y., Cheng, J., Zhu, S., Qiao, Z., Yang, J.: Friction and wear properties of Al-20Si-5Fe-2Ni-graphite solid-lubricating composite at elevated temperatures. Tribol. Int. **122**, 228–235 (2018)
25. Omrani, E., Moghadam, A.D., Menezes, P.L., Rohatgi, P.K.: Influences of graphite reinforcement on the tribological properties of self-lubricating aluminum matrix composites for green tribology, sustainability, and energy efficiency—a review. Int. J. Adv. Manuf. Technol. **83**(1-4), 325–346 (2016)
26. Wu, S., Tian, S., Menezes, P.L., Xiong, G.: Carbon solid lubricants: role of different dimensions. Int. J. Adv. Manuf. Technol. (2020). https://doi.org/10.1007/s00170-020-05297-8
27. Bagde, P., Sapate, S.G., Khatirkar, R.K., Vashishtha, N.: Friction and abrasive wear behaviour of Al_2O_3-13TiO_2 and Al_2O_3-13TiO_2+Ni graphite coatings. Tribol. Int. **121**, 353–372 (2018). https://doi.org/10.1016/j.triboint.2018.01.067
28. Zhao, X., Li, S., Hou, G., An, Y., Zhou, H., Chen, J.: Influence of doping graphite on microstructure and tribological properties of plasma sprayed $3Al_2O_3$–$2SiO_2$ coating. Tribol. Int. **101**, 168–177 (2016). https://doi.org/10.1016/j.triboint.2016.04.028

29. Gutierrez-Gonzalez, C.F., Smirnov, A., Centeno, A., Fernández, A., Alonso, B., Rocha, V.G., Torrecillas, R., Zurutuza, A., Bartolome, J.F.: Wear behavior of graphene/alumina composite. Ceram. Int. **41**(6), 7434–7438 (2015). https://doi.org/10.1016/j.ceramint.2015.02.061
30. Zhang, C., Nieto, A., Agarwal, A.: Ultrathin graphene tribofilm formation during wear of Al_2O_3–graphene composites. Nanomater. Energy. **5**(1), 1–9 (2016)
31. Gutiérrez-Mora, F., Cano-Crespo, R., Rincón, A., Moreno, R., Domínguez-Rodríguez, A.: Friction and wear behavior of alumina-based graphene and CNFs composites. J. Eur. Ceram. Soc. **37**(12), 3805–3812 (2017). https://doi.org/10.1016/j.jeurceramsoc.2017.02.024
32. Kim, H.J., Lee, S.-M., Oh, Y.-S., Yang, Y.-H., Lim, Y.S., Yoon, D.H., Lee, C., Kim, J.-Y., Ruoff, R.S.: Unoxidized graphene/alumina nanocomposite: fracture-and wear-resistance effects of graphene on alumina matrix. Sci. Rep. **4**(1), 1–10 (2014)
33. Wang, K., Wang, Y., Fan, Z., Yan, J., Wei, T.: Preparation of graphene nanosheet/alumina composites by spark plasma sintering. Mater. Res. Bull. **46**(2), 315–318 (2011). https://doi.org/10.1016/j.materresbull.2010.11.005
34. Porwal, H., Tatarko, P., Grasso, S., Khaliq, J., Dlouhý, I., Reece, M.J.: Graphene reinforced alumina nano-composites. Carbon. **64**, 359–369 (2013). https://doi.org/10.1016/j.carbon.2013.07.086
35. Liu, J., Yan, H., Jiang, K.: Mechanical properties of graphene platelet-reinforced alumina ceramic composites. Ceram. Int. **39**(6), 6215–6221 (2013). https://doi.org/10.1016/j.ceramint.2013.01.041
36. Fan, Y., Jiang, W., Kawasaki, A.: Highly conductive few-layer graphene/Al_2O_3 nanocomposites with tunable charge carrier type. Adv. Funct. Mater. **22**(18), 3882–3889 (2012)
37. Centeno, A., Rocha, V.G., Alonso, B., Fernández, A., Gutierrez-Gonzalez, C.F., Torrecillas, R., Zurutuza, A.: Graphene for tough and electroconductive alumina ceramics. J. Eur. Ceram. Soc. **33**(15), 3201–3210 (2013). https://doi.org/10.1016/j.jeurceramsoc.2013.07.007
38. An, J.W., You, D.H., Lim, D.S.: Tribological properties of hot-pressed alumina–CNT composites. Wear. **255**(1), 677–681 (2003). https://doi.org/10.1016/S0043-1648(03)00216-3
39. Lim, D.S., You, D.H., Choi, H.J., Lim, S.H., Jang, H.: Effect of CNT distribution on tribological behavior of alumina–CNT composites. Wear. **259**(1), 539–544 (2005). https://doi.org/10.1016/j.wear.2005.02.031
40. Su, Y., Zhang, Y., Song, J., Hu, L.: Novel approach to the fabrication of an alumina-MoS_2 self-lubricating composite via the in situ synthesis of nanosized MoS_2. ACS Appl. Mater. Interfaces. **9**(36), 30263–30266 (2017)
41. Deng, J., Can, T., Sun, J.: Microstructure and mechanical properties of hot-pressed Al_2O_3/TiC ceramic composites with the additions of solid lubricants. Ceram. Int. **31**(2), 249–256 (2005). https://doi.org/10.1016/j.ceramint.2004.05.009
42. Murakami, T., Ouyang, J., Umeda, K., Sasaki, S., Yoneyama, Y.: High-temperature friction and wear properties of X-BaSO4 (X: Al_2O_3, NiAl) composites prepared by spark plasma sintering. Mater. Trans. **46**(2), 182–185 (2005)
43. Murakami, T., Ouyang, J.H., Sasaki, S., Umeda, K., Yoneyama, Y.: High-temperature tribological properties of spark-plasma-sintered Al_2O_3 composites containing barite-type structure sulfates. Tribol. Int. **40**(2), 246–253 (2007). https://doi.org/10.1016/j.triboint.2005.09.013
44. Kerkwijk, B., García, M., van Zyl, W.E., Winnubst, L., Mulder, E.J., Schipper, D.J., Verweij, H.: Friction behaviour of solid oxide lubricants as second phase in α-Al_2O_3 and stabilised ZrO_2 composites. Wear. **256**(1), 182–189 (2004). https://doi.org/10.1016/S0043-1648(03)00388-0
45. Qi, Y.-e., Zhang, Y.-S., Hu, L.-T.: High-temperature self-lubricated properties of Al_2O_3/Mo laminated composites. Wear. **280-281**, 1–4 (2012). https://doi.org/10.1016/j.wear.2012.01.010
46. Fang, Y., Fan, H., Song, J., Zhang, Y., Hu, L.: Surface engineering design of Al_2O_3/Mo self-lubricating structural ceramics-part II: continuous lubrication effects of a three-dimensional lubricating layer at temperatures from 25 to 800° C. Wear. **360**, 97–103 (2016)